Original Article

Angiotensin II Type 1 Receptor Antagonist and Angiotensin-Converting Enzyme Inhibitor Altered the Activation of Cu/Zn-Containing Superoxide Dismutase in the Heart of Stroke-Prone Spontaneously Hypertensive Rats

Masakazu TANAKA, Seiji UMEMOTO*, Shinji KAWAHARA, Makoto KUBO, Shinichi ITOH, Kyoko UMEJI, and Masunori MATSUZAKI

Although angiotensin II type 1 (AT1) receptor antagonists and angiotensin-converting enzyme (ACE) inhibitors are known to reduce both reactive oxygen species (ROS) generated by activated NAD(P)H oxidase and vascular remodeling in hypertension, the effects of AT1 receptor antagonists or ACE inhibitors on ROS-scavenging enzymes remain unclear. We hypothesized that AT1 receptor antagonists or ACE inhibitors may modulate vascular remodeling *via* superoxide dismutase (SOD) in hypertension. Male stroke-prone spontaneously hypertensive rats (SHRSP) were treated for 6 weeks with a vehicle, an AT1 receptor antagonist (E4177; 30 mg/kg/day), or an ACE inhibitor (cilazapril; 10 mg/kg/day). We evaluated protein expression using immunoblots, determined SOD activities with a spectrophotometric assay, and measured NAD(P)H oxidase activity by a luminescence assay. The two drugs showed equipotent effects on blood pressure, left ventricular hypertrophy and fibrosis, and endothelial NO synthase in the SHRSP hearts. The wall-to-lumen ratio of the intramyocardial arteries and the NAD(P)H oxidase essential subunit $p22^{phox}$ and its activity were significantly reduced, whereas Cu/Zu-containing SOD (Cu/ZnSOD) expression and activity were significantly increased in the SHRSP hearts. Furthermore, E4177 reduced vascular remodeling more than did cilazapril not only by reducing $p22^{phox}$ expression and NAD(P)H oxidase activity but also by upregulating the Cu/ZnSOD expression and its activity in the SHRSP hearts. Thus, both the AT1 receptor antagonist and the ACE inhibitor inhibited vascular remodeling and reduced ROS in SHRSP *via* not only a reduction in NAD(P)H oxidase but also an upregulation of Cu/ZnSOD. (*Hypertens Res* 2005; 28: 67–77)

***Key Words*: superoxide dismutase, angiotensin, vascular remodeling, stroke-prone spontaneously hypertensive rats, oxidative stress**

Introduction

Increased production of vascular reactive oxygen species (ROS), especially superoxide anion, contributes to functional and structural alterations in hypertension. By stimulating the angiotensin II (Ang II) type 1 (AT1) receptor, Ang II contributes to the overexpression of cytosolic proteins involved in the activation of NAD(P)H oxidase, which is a major source of superoxide production (*1*, *2*). Overexpression of these

From the Department of Cardiovascular Medicine, Yamaguchi University Graduate School of Medicine, Ube, Japan; and *Pharmaceutical Clinical Research Center, Yamaguchi University Hospital, Ube, Japan.

This study was supported in part by grants from Eisai Co., Ltd. and the Takeda Science Foundation.

Address for Reprints: Masunori Matsuzaki, M.D., Ph.D., Department of Cardiovascular Medicine, Yamaguchi University Graduate School of Medicine, 1−1−1 Minamikogushi, Ube 755−8505, Japan. E-mail: masunori@yamaguchi-u.ac.jp

Received March 10, 2004; Accepted in revised form September 30, 2004.

cytosolic proteins might lead to vascular hypertrophy and remodeling in hypertension (*1*, *2*), and the AT1 receptor antagonist reduces overall oxidative stress in hypertensive patients independently of its effects on blood pressure (*3*). Conversely, enzyme superoxide dismutase (SOD) is a primary cellular defense against ROS. Three SOD isozymes, Cu/Zu-containing SOD (Cu/ZnSOD), manganese SOD (MnSOD), and extracellular SOD (ecSOD), have been identified, with Cu/ZnSOD being localized in the cytosol, MnSOD in mitochondria, and ecSOD in extracellular spaces. The predominant SOD activity in rat peripheral vessels is attributed to Cu/ZnSOD (*4*, *5*). Exposure to oxidative stress induced by the activation of NAD(P)H oxidase may exhaust the antioxidative capacity of the heart. In contrast, the increased activity of NAD(P)H oxidase is attenuated by increased activation of SOD induced by the administration of antioxidants in stroke-prone spontaneously hypertensive rats (SHRSP) (*6*), indicating that upregulation of antioxidant enzymes might reduce oxidative stress, improve vascular function and structure, and prevent the progression of hypertension in SHRSP.

Despite the many studies on the beneficial effects of angiotensin-converting enzyme (ACE) inhibitors and AT1 receptor antagonists on the vascular structure of intramyocardial arteries and oxidative stress in hypertension (*1*, *2*), the effects of AT1 receptor antagonists and ACE inhibitors on ROS-scavenging enzymes remain unclear. In this study, we assessed the hypothesis that AT1 receptor antagonists or ACE inhibitors might modulate vascular remodeling in the intramyocardial arteries of SHRSP *via* ROS-scavenging enzymes such as SOD.

Methods

The Ethics Committee for Animal Experimentation at the Yamaguchi University School of Medicine approved the experimental protocol used in this study. Experiments were performed according to the Guidelines for Animal Experimentation at the Yamaguchi University School of Medicine, and according to law No. 105 and notification No. 6 of the Japanese government.

Chemicals and Antibodies

The AT1 receptor antagonist E4177 and the ACE inhibitor cilazapril were provided by Eisai Co., Ltd. (Tokyo, Japan). The following were used in the immunofluorescence study and immunoblots: mouse monoclonal antibodies against human α-smooth muscle (SM) actin (Dako Cytomation Co., Ltd., Kyoto, Japan), human MnSOD (Chemicon International, Temecula, USA), human endothelial NO synthase (eNOS) (BD Transduction Laboratories, San Diego, USA), goat polyclonal antibodies against human $p22^{phox}$, Cu/ZnSOD, and calponin-1 (Santa Cruz Biotech, Santa Cruz, USA), horseradish peroxidase (HRP)-rabbit anti-goat and anti-mouse IgG, FITC-conjugated rabbit anti-mouse IgG (Zymed Laboratories, San Francisco, USA), and TRITC-conjugated rabbit anti-goat IgG (P.A.R.I.S., Compiègne, France).

Experimental Protocol

Twelve-week-old male Wistar-Kyoto rats (WKY group; $n=20$) and SHRSP ($n=60$) were obtained from Charles River Japan (Yokohama, Japan). SHRSP were randomized into three groups and treated for 6 weeks with a vehicle (SHRSP group; $n=20$), cilazapril (10 mg/kg/day, cilazapril group; $n=20$), or E4177 (30 mg/kg/day, E4177 group; $n=20$). The doses used in the experiments were determined according to Matsumoto *et al*. (*7*). Without anesthetizing the rats, we determined their systolic blood pressure (SBP) and heart rate by tail-cuff plethysmography. After the 6-week treatment period, rats were weighed and euthanized with a sodium pentobarbital overdose, and hearts were excised and weighed. Some of the excised hearts were perfused and fixed with heparinized saline followed by Bouin's solution *via* retrograde infusion into the ascending aorta at a pressure of 90 mmHg (*8*), and then paraffin-embedded 4- m slices were stained with Sirius red for histological analysis. The left ventricles of the other hearts were separated, washed with heparinized saline, weighed, and cut into three pieces perpendicular to the long axis. A piece of the middle portion of the heart tissue from each heart was snap-frozen with optimal cutting temperature (O.C.T.) compound in liquid nitrogen to obtain fresh-frozen, 4- m-thick sections for immunofluorescent staining. The rest of the apex-side heart tissues were frozen in liquid nitrogen and stored at −80°C until use for immunoblotting. The remaining base-side heart tissues were not used for the study, as we wanted to avoid contaminating the epicardial large coronary arteries.

Histological Analysis

To evaluate the coronary arterial wall thickness and perivascular fractional fibrosis, we scanned short-axis images of intramyocardial arteries at 200 magnification. In each heart, we evaluated the wall-to-lumen ratio (the medial thickness compared to the internal diameter) and a cross-sectional area of at least 10 intramyocardial arteries <150 m in diameter, as well as the perivascular collagen (the ratio of the collagen deposition area surrounding the vessel to the lumen area) and the interstitial collagen fraction (the ratio of the collagen deposition area in interstitial spaces and the corresponding left ventricular area) in the heart by analyzing Sirius red-stained sections under a microscope fitted with cross-polarization filters. All were evaluated in a blind fashion using a computer-assisted image analysis system with NIH Image software (ver. 1.62), according to the method of Baba *et al*. (*9*), and the mean value of each heart was used for statistical analysis.

Confocal Microscopy

We conducted dual immunolabeling using combinations of mouse monoclonal antibody against α-SM actin (dilution 1:100) and goat polyclonal antibodies against $p22^{phox}$ (dilution 1:100) or Cu/ZnSOD (dilution 1:100), or goat polyclonal antibodies against calponin-1 (dilution 1:50) and mouse monoclonal antibodies against MnSOD (dilution 1:200), to evaluate the colocalization of these proteins. After fixation, the sections were treated with 2.0% normal horse and 5.0% normal sheep serum (Vector Laboratories, Burlingame, USA) in phosphate-buffered saline for 30 min at room temperature, followed by incubation overnight at 4°C with the two primary antibodies applied together. The sections were then incubated for 1 h at room temperature with a mixture of the two secondary antibodies, FITC-conjugated rabbit anti-mouse IgG (dilution 1:100 or 200) and TRITC-conjugated rabbit anti-goat IgG (dilution 1:100). The sections were washed with three changes of phosphate-buffered saline, mounted in glycerol, and then examined by confocal microscopy with a laser scanning confocal fluorescence microscope (LSM510; Carl Zeiss, Inc., Jena, Germany) equipped with argon and helium-neon laser sources. Excitation wavelengths of 488 nm for FITC and 543 nm for TRITC were used to generate fluorescence emissions in green and red, respectively.

Immunoblotting

Immunoblots were performed as previously described (*10*). The $p22^{phox}$, Cu/ZnSOD, and MnSOD were separated by sodium dodecyl sulfate (SDS) -15% polyacrylamide gel electrophoresis (PAGE), and eNOS was separated on SDS-10% PAGE. Primary antibodies against $p22^{phox}$ and Cu/ZnSOD were used at a dilution of 1:500; MnSOD and eNOS were used at a dilution of 1:1000. Equal amounts of protein of total tissue homogenate from heart tissue were applied in each well ($p22^{phox}$, 40 g; Cu/ZnSOD, 30 g; MnSOD, 12 g; eNOS, 20 g) and then electroblotted and detected with the ECL system (Amersham Biosciences, Buckinghamshire, UK). After immunoblotting, the film was scanned and densitometric analyses were performed using NIH Image software (ver. 1.62).

Measurement of Oxidative Stress

Myocardial oxidative stress was estimated by measuring both 8-*iso*-prostaglandin $F_{2\alpha}$ (8-*iso*-$PGF_{2\alpha}$) and thiobarbituric acid reactive substances (TBARS). The level of 8-*iso*-$PGF_{2\alpha}$ was measured using an enzyme-linked immunoassay kit (Cayman Chemicals, Ann Arbor, USA) (*11*). Briefly, cardiac tissues were homogenized and then protected by the addition of indomethacin (0.001% w/v) to prevent *in vitro* formation of prostanoids due to any leukocyte contamination. Tissues were hydrolyzed with the appropriate excess volume of 2 mol/l KOH at 45°C for 2 h. After hydrolysis, samples were cooled and treated with an equal volume of 2 mol/l HCl, and the neutralized samples were then centrifuged at 3,000 rpm for 20 min. Using 8-*iso*-$PGF_{2\alpha}$ as the standard, we calculated the level of 8-*iso*-$PGF_{2\alpha}$ as pg/mg wet tissue.

TBARS levels were determined by a colorimetric method (Wako Pure Chemicals, Tokyo, Japan) (*12*). Briefly, cardiac tissue was homogenized in 6.5% trichloroacetic acid (TCA), and a reagent containing 15% TCA, 0.375% thiobarbituric acid, and 0.25% HCl was added. The sample was then mixed thoroughly, heated for 15 min in a boiling water bath, cooled, and centrifuged at 2,000 rpm; the absorbance of the supernatant was then measured at 535 nm against a blank that contained all reagents except the tissue homogenate. Using malondialdehyde as a standard, we calculated TBARS as nmol/mg wet tissue.

Measurement of SOD Activity

SOD activities were determined based on the SOD-mediated increase in the rate of autoxidation of 5,6,6a,11b-tetrahydro-3,9,10-trihydroxybenzo[c]fluorine in aqueous alkaline solution to yield a chromophore with maximum absorbance at 525 nm with a spectrophotometric assay (OxisResearch, Portland, USA) (*13*). Briefly, heart tissues were washed with 0.9% NaCl containing heparin to remove red blood cells, followed by homogenization and centrifugation. Next, 40 l of tissue homogenate was added to 900 l of 2-amino-2-methyl-1,3-propanediol containing boric acid and diethylenetriaminepentaacetic acid (DTPA) (pH 8.8), and then 30 l of 1,4,6-trimethyl-2,2-vinylpyridinium trifluoromethanesulfonate in HCl was added. The mixture was briefly vortexed and then incubated at 37°C for 1 min. We added 30 l of 5,6,6a,11b-tetrahydro-3,9,10-trihydroxybenzo[c]fluorine in HCl containing DTPA and ethanol, and immediately measured the absorbance at 525 nm spectrophotometrically. The SOD activity was determined from the ratio of the autoxidation rates in the presence and absence of SOD. Absolute ethanol/chloroform, 62.5/37.5 (v/v), was used to inactivate MnSOD and to specifically measure Cu/ZnSOD activity according to the manufacturer's recommendations.

Measurement of NAD(P)H Oxidase Activity

NAD(P)H oxidase activities were determined by a luminescence assay (*14*). Briefly, heart tissues were placed in a chilled, modified Krebs-HEPES buffer (99 mmol/l NaCl, 4.7 mmol/l KCl, 1.9 mmol/l $CaCl_2$, 1.2 mmol/l $MgSO_4$, 1.0 mmol/l K_2HPO_4, 25 mmol/l $NaHCO_3$, 20 mmol/l Na-HEPES, and 11 mmol/l glucose, pH 7.4). A 10% (w/v) tissue homogenate in a 50 mmol/l phosphate buffer was subjected to centrifugation at 1,000 *g* for 10 min to remove unbroken cells and debris. An aliquot was kept for protein determination, and supernatants (25 l) were assayed immediately for superoxide production. A luminescence assay was performed in a 50 mmol/l phosphate buffer, pH 7.0, containing 1 mmol/l

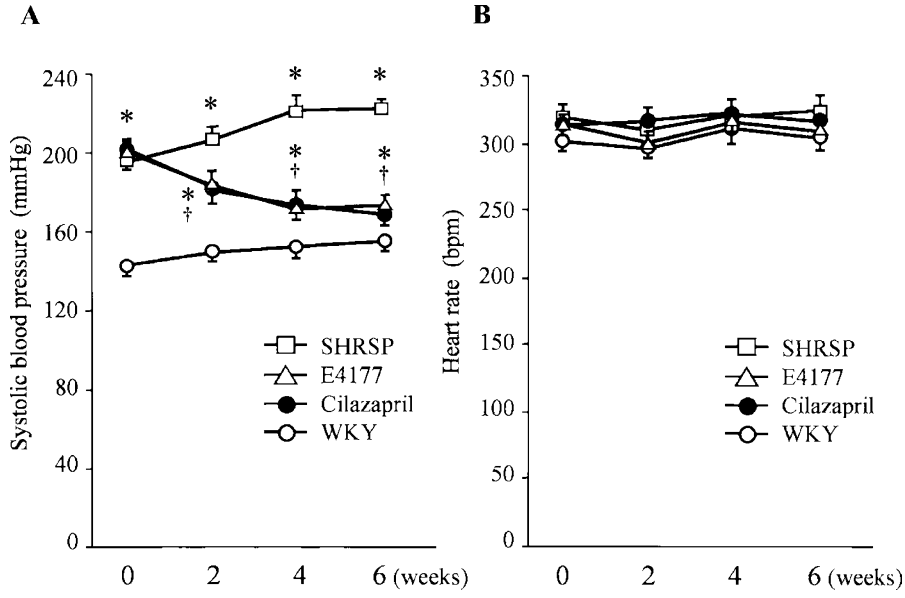

Fig. 1. *Systolic blood pressure and heart rate in the WKY, vehicle SHRSP, cilazapril, and E4177 groups. Bars indicate SEM.* *p < *0.01* vs. *the WKY group,* †p < *0.01* vs. *the vehicle SHRSP group. Experiments,* n = *5–7.*

EGTA, 150 mmol/l sucrose, 500 mol/l lucigenin (bis-*N*-methylacridinium nitrate) as the electron acceptor, and 100 mol/l NAD(P)H as the substrate (final volume 225 l), all of which was poured into a 96-well microplate. This concentration fell well within the linear range of the assay (1 mol/l to 10 mmol/l for NAD(P)H), and NAD(P)H was not rate-limiting over the initial course of the assay. No activity could be measured in the absence of NAD(P)H. After dark adaptation, background counts were recorded and a tissue homogenate was added to the microplate. The lucigenin count was then recorded every 15 s for 10 min, and the respective background counts (without tissue homogenate) were subtracted from tissue homogenate readings. The lucigenin count was expressed as counts per second per milligram of the tissue homogenate.

Statistical Analysis

All values were expressed as the means±SEM. The experimental groups were compared with ANOVA followed by Scheffe's multiple comparisons; values of $p<0.05$ were considered statistically significant.

Results

Throughout the experiments, SBP in the vehicle SHRSP group was significantly higher than that in the WKY group. The two drugs induced equivalent and significant reductions in SBP compared to the levels in the SHRSP group. However, both the cilazapril and E4177 groups showed significantly higher SBP than did the WKY group (Fig. 1A). Heart rates were unaltered among the four groups throughout the experiments (Fig. 1B). Body weight was greater in the WKY group than in the three SHRSP groups, but there was no difference in body weight among the three SHRSP groups. Left ventricular weight/body weight in the three SHRSP groups was significantly greater than that in the WKY group. In addition, compared to the vehicle SHRSP group, the two drug-treated SHRSP groups showed significant and equal reductions in left ventricular weight/body weight (Table 1).

Table 1. BW and LVW in 18-Week-Old Rats

Parameter	WKY	SHRSP	Cilazapril	E4177
BW (g)	389±11	295±5*	293±4*	297±4*
LVW (mg)	843±13	857±14	768±15*,†	735±10*,†
LVW/BW (mg/g)	2.07±0.1	2.76±0.1*	2.48±0.1*,‡	2.38±0.1*,‡

Values are the mean±SEM. WKY and SHRSP were treated with vehicle, cilazapril (10 mg/kg/day), or E4177 (30 mg/kg/day) for 6 weeks. *$p<0.01$ *vs.* the WKY groups, †$p<0.01$, ‡$p<0.05$ *vs.* the SHRSP group. BW, body weight; LVW, left ventricular weight; WKY, Wistar-Kyoto rats; SHRSP, stroke-prone spontaneously hypertensive rats. Experiments, $n=8$.

Figure 2 shows a representative micrograph of the effects of cilazapril and E4177 on vascular remodeling and perivascular collagen deposition in an intramyocardial artery, and Table 2 summarizes the quantitative analysis of the wall-to-lumen ratio and the cardiac collagen deposition in rat hearts. The wall-to-lumen ratio and cross-sectional area of the intramyocardial arteries in the vehicle SHRSP group were significantly greater than those in the WKY group. Both these parameters were significantly lower in the two drug-treated groups than in the vehicle SHRSP group. Furthermore, E4177 reduced the

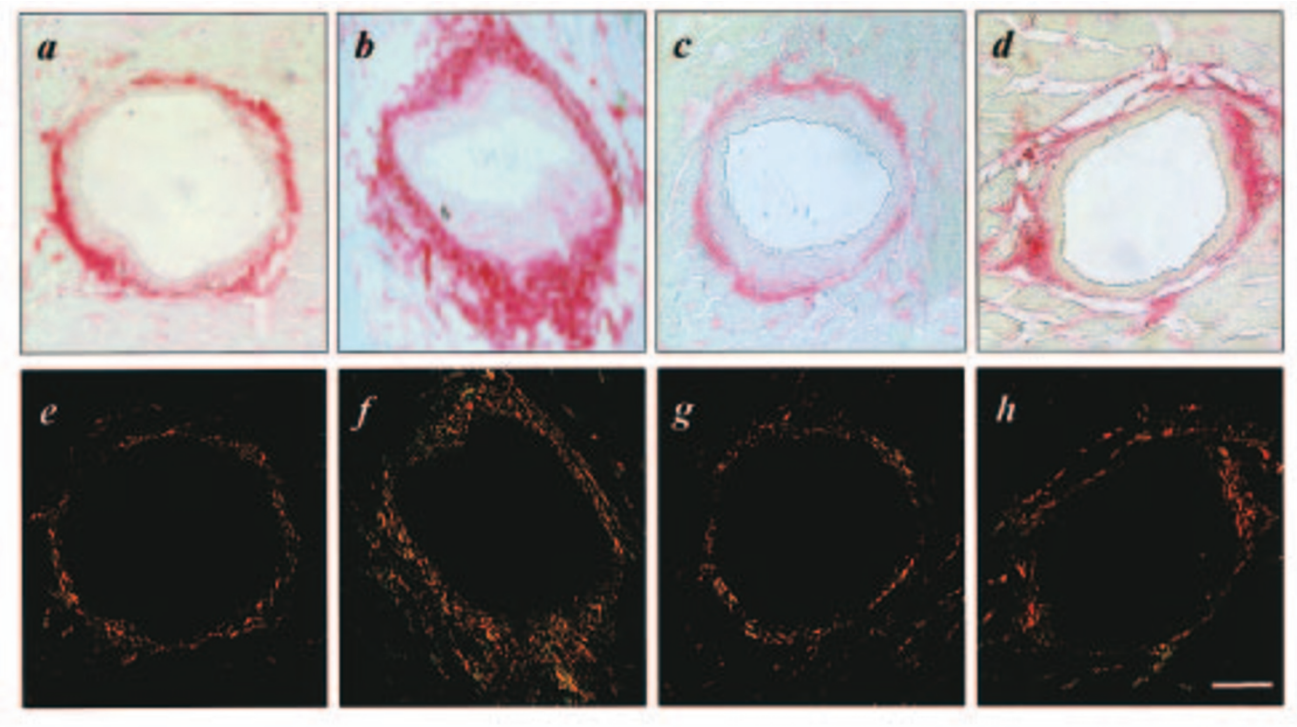

Fig. 2. *Representative micrograph of the effects of cilazapril and E4177 on vascular remodeling and perivascular collagen deposition in an intramyocardial artery. The sections were stained with Sirius red F3BA (a–d) and viewed through a polarized-light microscope (e–h). Arteries of WKY (a and e) and SHRSP treated with vehicle (b and f), cilazapril (c and g), and E4177 (d and h) are shown. Bar, 50 m.*

Table 2. Wall-to-Lumen Ratio and Cross-Sectional Area of Intramyocardial Arteries, and Cardiac Collagen Area in 18-Week-Old Rats

Parameter	WKY	SHRSP	Cilazapril	E4177
Wall-to-lumen ratio	0.11±0.01	0.30±0.02*	0.22±0.02*,†	0.12±0.01†,§
Cross-sectional area (m^2/g)	9.4±1.9	53.0±4.8*	28.4±3.6*,†	13.1±1.6†,§
Perivascular collagen	0.7±0.1	2.0±0.2*	0.9±0.2†	0.8±0.2†
Interstitial collagen fraction (%)	1.1±0.2	2.5±0.3*	1.4±0.2‡	0.8±0.1†

Values are the mean±SEM. WKY and SHRSP were treated with vehicle, cilazapril (10 mg/kg/day), and E4177 (30 mg/kg/day) for 6 weeks. *$p<0.01$, *vs.* the WKY groups, †$p<0.01$, ‡$p<0.05$ *vs.* the SHRSP group, §$p<0.01$ *vs.* the cilazapril group. WKY, Wistar-Kyoto rats; SHRSP, stroke-prone spontaneously hypertensive rats. Experiments, $n=8$.

wall-to-lumen ratio and cross-sectional area more than did cilazapril in SHRSP, and the ratio by E4177 reached the same level as was present in the WKY group. Both the perivascular and interstitial collagen deposition were significantly higher in the vehicle SHRSP group than in the WKY group. Both drugs significantly reduced the perivascular and interstitial collagen deposition compared with those in the vehicle SHRSP group, with no significant differences in values among the WKY group and the two drug-treated SHRSP groups.

Figure 3 shows that the vehicle SHRSP group had significantly higher cardiac levels of both 8-*iso*-$PGF_{2\alpha}$ and TBARS than did the WKY group. Both cilazapril and E4177 significantly inhibited the increase in both 8-*iso*-$PGF_{2\alpha}$ and TBARS in the SHRSP hearts, although the levels of 8-*iso*-$PGF_{2\alpha}$ in the cilazapril group were significantly higher than those in the WKY group. Furthermore, there was a significant difference between the ability of cilazapril and that of E4177 to prevent a rise in both 8-*iso*-$PGF_{2\alpha}$ and TBARS levels in the SHRSP hearts: E4177 almost entirely abolished the increases in both oxidative stress parameters, resulting in levels almost identical to those in the WKY group.

Figure 4A shows that $p22^{phox}$ expression was significantly upregulated in the vehicle SHRSP group compared with that in the WKY group. Both cilazapril and E4177 significantly downregulated $p22^{phox}$ expression compared with that in the vehicle SHRSP group. The E4177 group showed expression at almost the same level as that of the WKY group, whereas the level of $p22^{phox}$ expression in the cilazapril group was sig-

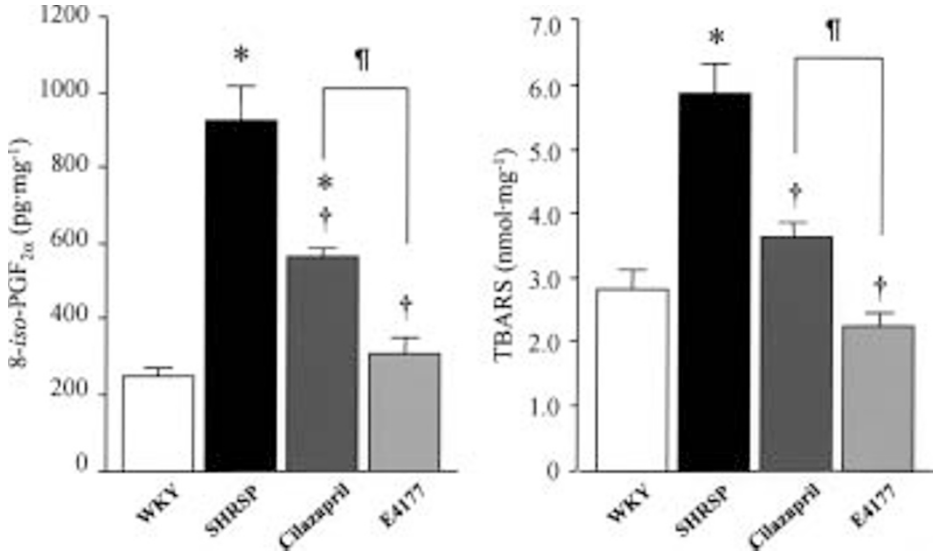

Fig. 3. *Levels of 8-*iso*-$PGF_{2\alpha}$ and TBARS in rat hearts. Bars indicate SEM.* *p < 0.01* vs. *the WKY group,* †*p < 0.01* vs. *the vehicle SHRSP group,* ¶*p < 0.05* vs. *the cilazapril group. Experiments,* n = *8. 8-*iso*-$PGF_{2\alpha}$, 8-*iso*-prostaglandin $F_{2\alpha}$; TBARS, thiobarbituric acid reactive substances.*

nificantly higher than that of the WKY group. Inversely, Cu/ZnSOD expression was significantly downregulated in the vehicle SHRSP group compared with that in the WKY group. Compared to that in the vehicle SHRSP group, Cu/ZnSOD expression was significantly upregulated in both the cilazapril and E4177 groups, to levels almost equivalent to that in the WKY group. Furthermore, significant differences were seen between the cilazapril and E4177 groups in Cu/ZnSOD expression in SHRSP hearts. MnSOD expression in the heart was unaltered in each of the four groups.

Figure 4B shows the results of dual immunofluorescent staining of $p22^{phox}$, Cu/Zn-, or MnSOD, as well as α-SM actin and calponin 1 expression in the rat heart; it can be seen that $p22^{phox}$ was mainly localized not only in the media but also in the perivascular area of intramyocardial arteries in the vehicle SHRSP group, whereas $p22^{phox}$ was mainly localized only in the media of the intramyocardial arteries in the WKY group. Cardiac myocytes scarcely expressed $p22^{phox}$ in rat hearts. In contrast, Cu/ZnSOD and MnSOD were relatively and uniformly localized in the media of the intramyocardial arteries,

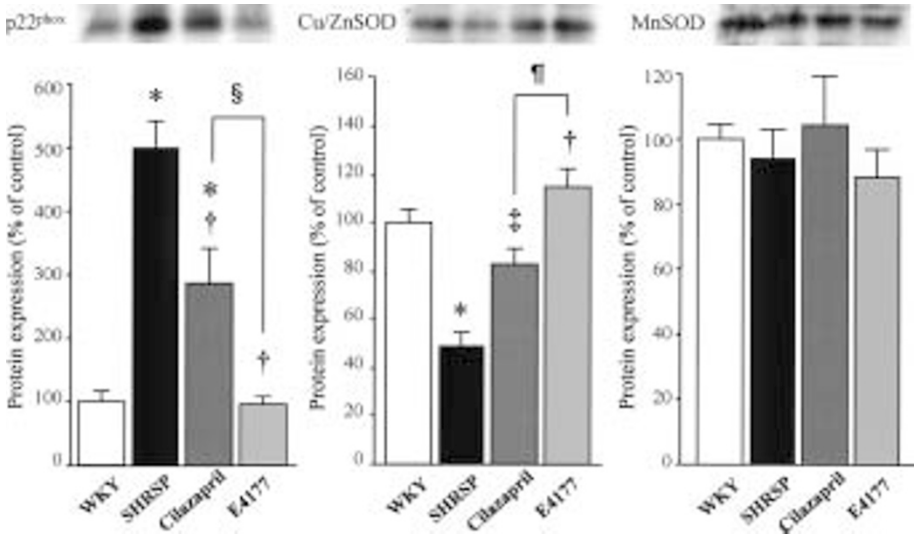

Fig. 4A. *Quantitative analysis of $p22^{phox}$, Cu/Zn-, and MnSOD expression in rat hearts. Bars indicate SEM.* *p < 0.01 vs. *the WKY group,* †*p < 0.01,* ‡*p < 0.05* vs. *the vehicle SHRSP group,* §*p < 0.01,* ¶*p < 0.05* vs. *the cilazapril group. Experiments,* n = *8.*

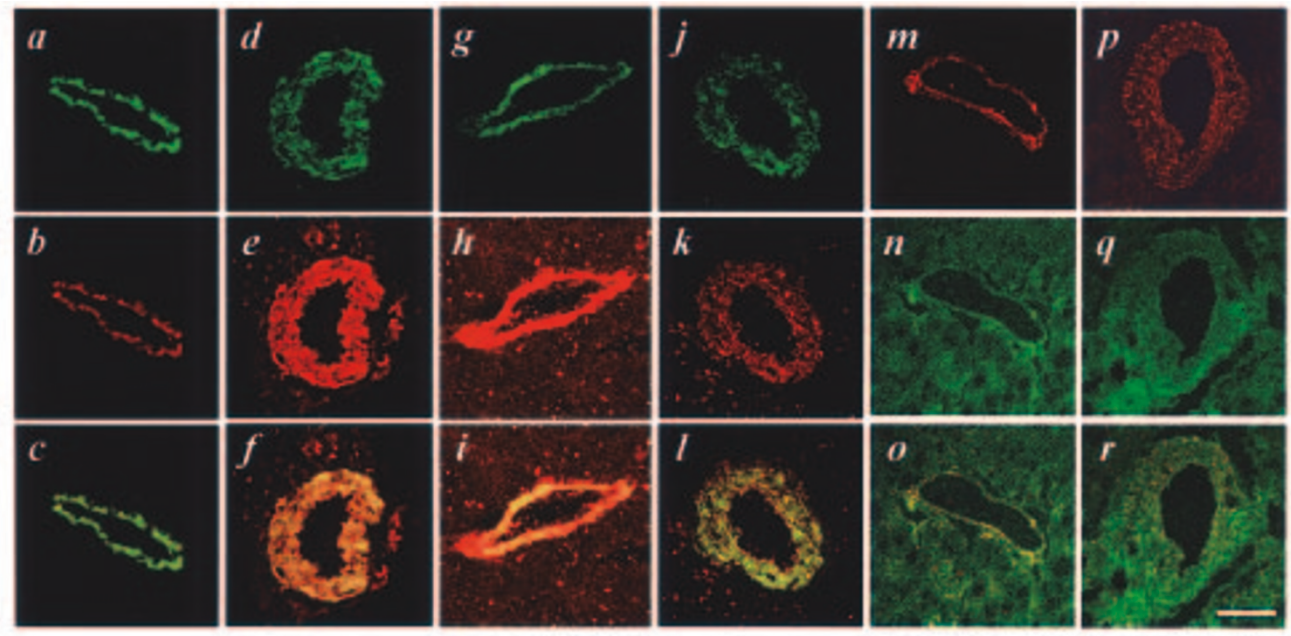

Fig. 4B. *Confocal microscopic analyses of the localization of p22^{phox}, Cu/Zn-, and MnSOD in an intramyocardial artery in rat hearts. Tissues were labeled with specific antibodies against α-SM actin (a, d, g, and j), calponin 1 (m and p), p22^{phox} (b and e), Cu/ZnSOD (h and k), or MnSOD (n and q) in rat hearts. Arteries of WKY (a–c, g–i, and m–o) and SHRSP (d–f, j–l, and p–r) are shown. Merged images: α-SM actin with p22^{phox} (c and f), Cu/ZnSOD (i and l) and calponin 1 with MnSOD (o and r). Bar, 50 m.*

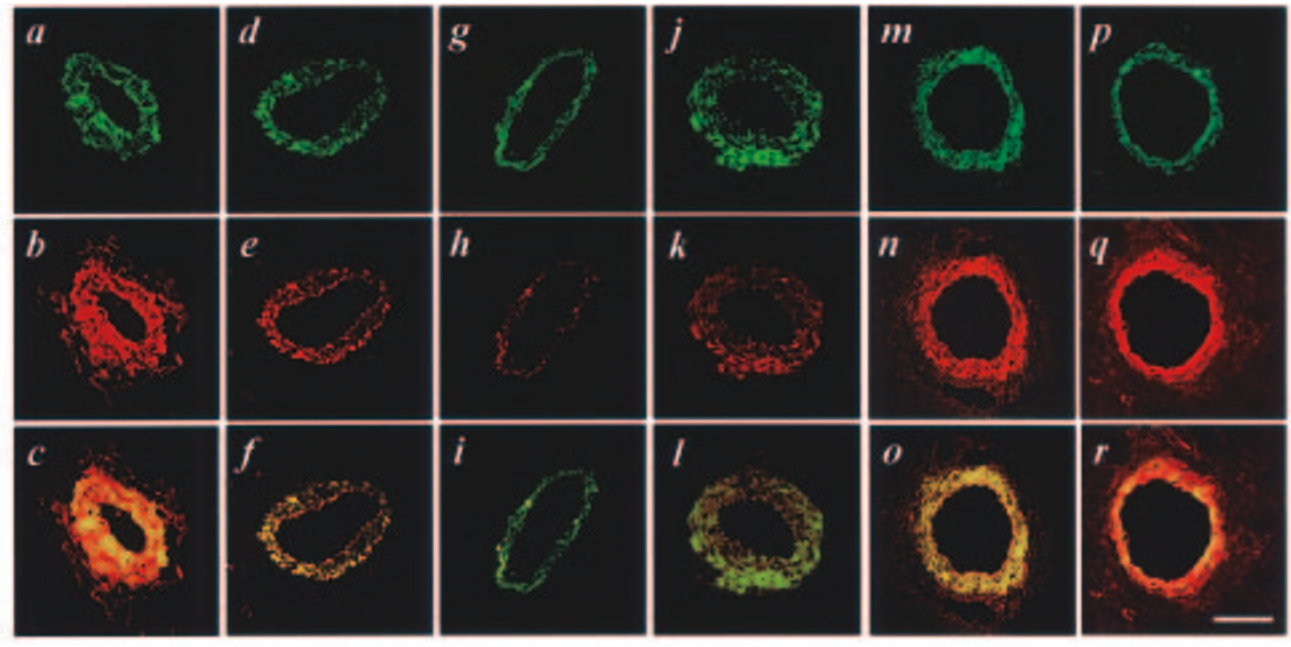

Fig. 4C. *Confocal microscopic analyses of the effects of cilazapril and E4177 on p22^{phox} and Cu/ZnSOD in an intramyocardial artery in SHRSP hearts. Tissues were labeled with specific antibodies against α-SM actin (a, d, g, j, m, and p), p22^{phox} (b, e, and h), and Cu/ZnSOD (k, n, and q) in SHRSP hearts. Arteries from animals in the vehicle SHRSP (a–c and j–l), cilazapril (d–f and m–o), and E4177 (g–i and p–r) groups are shown. Merged images: α-SM actin with p22^{phox} (c, f, and i) and Cu/ZnSOD (l, o, and r). Bar, 50 m.*

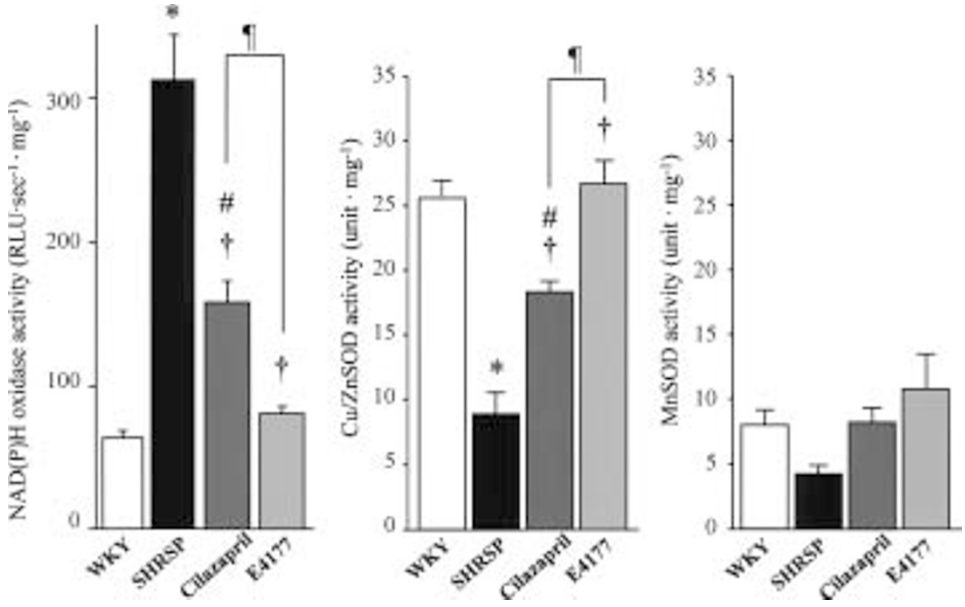

Fig. 5. *Quantitative analysis of NAD(P)H oxidase activity and Cu/Zn- and MnSOD activity in rat hearts. Bars indicate SEM.* *$p < 0.01$, #$p < 0.05$ vs. *the WKY group,* †$p < 0.01$ vs. *the vehicle SHRSP group,* ¶$p < 0.05$ vs. *the cilazapril group. Experiments,* $n = 4–5$.

but they were also found in cardiac myocytes in both the WKY and vehicle SHRSP groups. However, Cu/ZnSOD expression in cardiac myocytes was higher in the WKY group than in the vehicle SHRSP group.

Figure 4C shows the results of dual immunofluorescent staining of $p22^{phox}$ and Cu/ZnSOD, as well as α-SM actin expression in the SHRSP hearts. Both cilazapril and E4177 inhibited $p22^{phox}$ expression in the perivascular area and media of the intramyocardial arteries in the SHRSP heart, whereas Cu/ZnSOD expression was increased primarily in the perivascular area and media of the intramyocardial arteries as well as in cardiac myocytes of the SHRSP heart by the administration of cilazapril and E4177.

Figure 5 shows the results of the quantitative analysis of both NAD(P)H oxidase and SOD activities in rat hearts. NAD(P)H oxidase activity was significantly upregulated in the vehicle SHRSP group compared with the WKY group. Both cilazapril and E4177 significantly downregulated NAD(P)H oxidase activity compared to that in the vehicle SHRSP group. The E4177 group showed NAD(P)H oxidase activity at almost the same level as that of the WKY group, whereas the levels of NAD(P)H oxidase activity in the cilazapril group were significantly higher than those of the WKY group. In addition, there were significant differences in NAD(P)H oxidase activity in SHRSP hearts between the cilazapril and E4177 groups. Inversely, Cu/ZnSOD activity was significantly downregulated in the vehicle SHRSP group compared with that in the WKY group. Compared to that in the vehicle SHRSP group, Cu/ZnSOD activity in SHRSP hearts was significantly upregulated in both the cilazapril and E4177 groups. Cu/ZnSOD activity in the E4177 group improved to almost the same level as that of the WKY group, whereas Cu/ZnSOD activity in the cilazapril group was significantly lower than that of the WKY group. In addition, there were significant differences between the cilazapril and E4177 groups in Cu/ZnSOD activity in SHRSP hearts. MnSOD activity in the heart was not significantly different among the four groups.

The levels of eNOS expression in the rat heart were significantly downregulated in the vehicle SHRSP group compared with those in the WKY group (Fig. 6). Both cilazapril and E4177 caused significant upregulation of eNOS expression in SHRSP hearts, resulting in eNOS expression levels equivalent to those in the WKY hearts, while there were no differences in the degree of upregulation of eNOS expression in hearts between the two drug-treated SHRSP groups.

Discussion

The blood pressure-lowering actions of cilazapril and E4177 were accompanied by decreases in both oxidative stress and vascular hypertrophy, indicating that these processes are redox-sensitive in SHRSP (*6*), and equihypotensive effects of the two drugs were observed with the doses used in our study. We therefore conclude that the different mechanisms by which E4177 and cilazapril influence these processes could be related to the direct inhibiting action of ROS-generating enzyme systems and/or the upregulation of ROS-scavenging enzyme systems, as E4177 and cilazapril belong to two different classes of drugs. There are some differences in the mech-

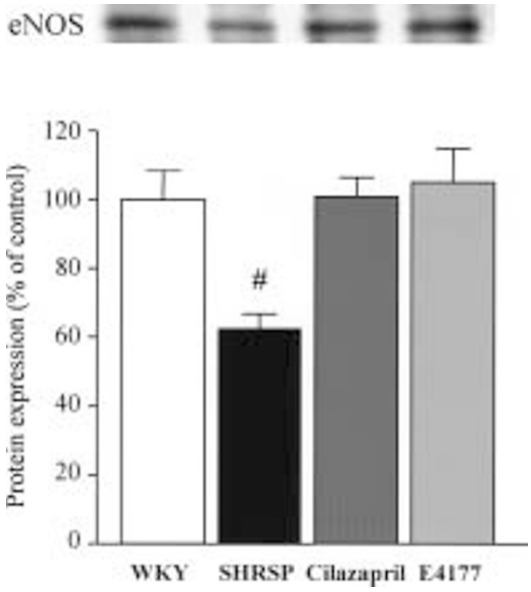

Fig. 6. *Quantitative analysis of eNOS expression in rat hearts. Bars indicate SEM.* $^{\#}p < 0.05$ vs. *the WKY, cilazapril, and E4177 groups. Experiments,* $n = 8$.

anisms for blocking the renin-angiotensin system by the two drugs: cilazapril blocks Ang II formation, and hence less Ang II is available to stimulate both the AT1 and Ang II type 2 (AT2) receptors, whereas E4177 selectively blocks the AT1 receptor, causing the upregulation of Ang II formation and the stimulation of AT2 receptors. Activation of AT1 receptor by Ang II leads to phosphorylation of $p47^{phox}$ and subsequent translocation of $p47^{phox}$ to the membrane through the activation of phospholipase D, protein kinase C, and c-Src tyrosine kinase (*2*). This process promotes phosphorylated $p47^{phox}$ binding to the membrane component $p22^{phox}$ to activate NAD(P)H oxidase (*2*). In addition, it has been reported that the AT2 receptor function might be impaired in SHRSP, which could be responsible for the inappropriate progression of vascular remodeling in hypertension (*15*, *16*), indicating that involvement of the AT2 receptor might be less than previously thought. These observations also indicate that the AT1 receptor, but not the AT2 receptor, plays a crucial role in vascular remodeling and NAD(P)H oxidase activity. Furthermore, aldosterone production in the vasculature may be involved in the results of our experiments. It has been shown that aldosterone is produced in the heart and blood vessels. The biological effects of aldosterone are mediated by the cardiac and vascular mineralocorticoid receptors, and the direct actions of Ang II, such as that of vascular remodeling *via* oxidative stress and inflammation of the vascular wall and heart, may be mediated in part by aldosterone (*17*). Furthermore, it has recently been suggested that Src activation by aldosterone is mediated through the mineralocorticoid receptor (*18*). Taken together with the previous report (*2*), these results suggest that NAD(P)H oxidase activity is regulated to some extent by aldosterone. Aldosterone selectivity in mineralocorticoid target tissues is primarily due to 11β-hydroxysteroid dehydrogenase, and diminished activity in resistance vessels of genetically hypertensive rats has also been shown (*19*). In the present study, we did not evaluate the effects of aldosterone on vascular remodeling in the SHRSP heart. However, recent studies have demonstrated that plasma aldosterone levels as well as plasma Ang II levels are not chronically suppressed by ACE inhibitors (*20*), whereas the AT1 receptor antagonist shows no evidence of aldosterone escape (*21*), suggesting that the effects of aldosterone escape in E4177 on vascular remodeling might be less than those in cilazapril.

Our immunofluorescence study has demonstrated that NAD(P)H oxidase assessed by the essential subunit of this enzyme, $p22^{phox}$, is primarily expressed in the media of intramyocardial arteries and the perivascular area in the heart, and that both cilazapril and E4177 downregulate the expression of $p22^{phox}$ in the perivascular area and the media of intramyocardial arteries in SHRSP hearts. Moreover, a significant difference in NAD(P)H oxidase activity as well as $p22^{phox}$ expression in SHRSP hearts was observed between the cilazapril and E4177 groups with the doses used in this experiment. Because NAD(P)H oxidase is the major source of superoxide anion in vascular cells (*1*), decreased activation of this enzyme by administration of the two drugs would result in reduced generation of superoxide anions in SHRSP hearts. In addition, both drugs were also found to reduce oxidative stress not only by decreasing NAD(P)H oxidase activity but also by selectively increasing Cu/ZnSOD expression and its activity, primarily in the perivascular area and media of the intramyocardial arteries, and also in cardiac myocytes of the SHRSP hearts. Furthermore, E4177 was found to reduce the concentrations of ROS to the same levels as those in the WKY group more efficiently than did cilazapril in SHRSP hearts, even though the E4177 group showed significantly higher SBP than the WKY group. These findings suggest that enhanced activation of Cu/ZnSOD in SHRSP hearts would lead to a further decrease in superoxide anion concentrations, and that E4177 may have additional benefits for the reduction of ROS in SHRSP hearts beyond the lowering of blood pressure. In earlier studies, antioxidants or chronic treatment with a SOD mimetic have been found to reduce oxidative stress, improve vascular function and structure, and prevent the progression of hypertension in SHRSP by altering the activation of vascular NAD(P)H oxidase and Cu/ZnSOD (*6*, *22*). Furthermore, administration of Cu/ZnSOD within the vessel wall has been found to normalize the blood pressure of genetically hypertensive rats (*23*). It is also possible that both AT1 receptor antagonists and ACE inhibitors will improve endothelial function by accelerating the ROS-scavenging systems (*24*). Although we cannot elucidate which of the two ROS-related enzyme systems is more important, our results regarding the localization of Cu/ZnSOD and MnSOD in the rat heart are similar to those reported previously (*25*), and we observed, through comparisons between the two, that these

systems together could contribute to an overall reduction in the generation of ROS, improved oxidative status, and the inhibition of vascular remodeling of intramyocardial arteries in SHRSP. Our results are supported by Didion *et al*. (*26*), who clearly demonstrated that the selective loss of Cu/Zn-SOD results in increased superoxide and altered vascular responsiveness in both large arteries and microvessels in Cu/ZnSOD-deficient (Cu/ZnSOD$^{-/-}$) mice. The mechanisms by which E4177 and cilazapril influence Cu/ZnSOD are ill-defined, but the AT1 receptor might play an important role in the regulation of Cu/ZnSOD, based on the results observed in our study and those of an earlier report (*27*) which suggested that AT1 receptor function is involved in the regulation of Cu/ZnSOD. In addition, it has been reported that expression of the Cu/ZnSOD gene is induced by the inducible binding of peroxisome proliferators to peroxisome proliferator-activated receptors through the peroxisome proliferator-responsive element site, which is located between nt −797 and −786 of the 5′-flanking sequence of the rat Cu/ZnSOD gene (*28*), and that AT1 receptor antagonists induce peroxisome proliferators-activated receptor-γ activity (*29*). Taking the above together with our results, it is suggested that E4177 may upregulate Cu/ZnSOD activity through the activation of these processes in SHRSP hearts.

Increased vascular ROS production diminishes NO bioavailability and leads to endothelial dysfunction and vascular hypertrophy in hypertension (*30*). Although we did not measure NO activity in this study, it is possible that, even though cilazapril and E4177 had equipotent effects on the restoration of eNOS expression in SHRSP hearts, E4177 might provide additional benefits in terms of NO bioavailability. These processes could have been associated with attenuated vascular remodeling and reduced ROS in SHRSP *via* not only reductions in NAD(P)H oxidase levels but also upregulation of Cu/ZnSOD in our study.

In the present study, we did not examine the effects of E4177 and cilazapril on ROS-scavenging enzymes such as glutathione peroxidase and/or catalase in the rat heart (*31*). We cannot exclude the possibility that such ROS-scavenging enzymes as well as Cu/ZnSOD might affect ROS levels in the SHRSP heart. In addition, several reports have demonstrated that rat ecSOD is lacking in the vessel wall and is primarily present in plasma (*4*), and that ecSOD activity is quite low in the heart (*32*); as such, it is unlikely that ecSOD plays a critical role in the heart, although we cannot exclude the possibility that ecSOD in plasma could have influenced our results.

In summary, our study has demonstrated that E4177 and cilazapril might inhibit vascular remodeling in intramyocardial arteries of SHRSP *via* not only ROS-generating enzyme NAD(P)H oxidase but also through ROS-scavenging enzymes such as Cu/ZnSOD in the SHRSP heart. Although little is known about ROS-scavenging enzymes in hypertension *in vivo*, and further experiments will be necessary to examine the antioxidant properties of both agents, our findings provide a new view of hypertension and vascular remodeling, and present important information regarding the development of more effective therapies for hypertension.

Acknowledgements

We would like to thank Rie Ishihara and Kazuko Iwamoto for their excellent technical assistance and Dr. Tohru Fukai, Emory University, for his helpful discussions on ecSOD.

References

1. Griendling KK, Sorescu D, Lassegue B, Ushio-Fukai M: Modulation of protein kinase activity and gene expression by reactive oxygen species and their role in vascular physiology and pathophysiology. *Arterioscler Thromb Vasc Biol* 2000; **20**: 2175–2183.
2. Cai H, Griendling KK, Harrison DG: The vascular NAD(P)H oxidases as therapeutic targets in cardiovascular diseases. *Trends Pharmacol Sci* 2003; **24**: 471–478.
3. Dohi Y, Ohashi M, Sugiyama M, Takase H, Sato K, Ueda R: Candesartan reduces oxidative stress and inflammation in patients with essential hypertension. *Hypertens Res* 2003; **26**: 691–697.
4. Carlsson LM, Marklund SL, Edlund T: The rat extracellular superoxide dismutase dimer is converted to a tetramer by the exchange of a single amino acid. *Proc Natl Acad Sci USA* 1996; **93**: 5219–5222.
5. Fukai T, Folz RJ, Landmesser U, Harrison DG: Extracellular superoxide dismutase and cardiovascular disease. *Cardiovasc Res* 2002; **55**: 239–249.
6. Chen X, Touyz RM, Park JB, Schiffrin EL: Antioxidant effects of vitamins C and E are associated with altered activation of vascular NADPH oxidase and superoxide dismutase in stroke-prone SHR. *Hypertension* 2001; **38**: 606–611.
7. Matsumoto K, Morishita R, Moriguchi A, *et al*: Prevention of renal damage by angiotensin Ⅱ blockade, accompanied by increased renal hepatocyte growth factor in experimental hypertensive rats. *Hypertension* 1999; **34**: 279–284.
8. Young AA, Legrice IJ, Young MA, Smaill BH: Extended confocal microscopy of myocardial laminae and collagen network. *J Microsc* 1998; **192**: 139–150.
9. Baba HA, Iwai T, Bauer M, Irlbeck M, Schmid KW, Zimmer HG: Differential effects of angiotensin Ⅱ receptor blockade on pressure-induced left ventricular hypertrophy and fibrosis in rats. *J Mol Cell Cardiol* 1999; **31**: 445–455.
10. Fujii K, Umemoto S, Fujii A, Yonezawa T, Sakumura T, Matsuzaki M: Angiotensin Ⅱ type 1 receptor antagonist downregulates nonmuscle myosin heavy chains in spontaneously hypertensive rat aorta. *Hypertension* 1999; **33**: 975–980.
11. Hermann M, Camici G, Fratton A, *et al*: Differential effects of selective cyclooxygenase-2 inhibitors on endothelial function in salt-induced hypertension. *Circulation* 2003; **108**: 2308–2311.
12. Kikugawa K, Kojima T, Yamaki S, Kosugi H: Interpretation of the thiobarbituric acid reactivity of rat liver and brain homogenates in the presence of ferric ion and ethylenediaminetetraacetic acid. *Anal Biochem* 1992; **202**: 249–255.
13. Nebot C, Moutet M, Huet P, Xu JZ, Yadan JC, Chaudiere J: Spectrophotometric assay of superoxide dismutase activity

based on the activated autoxidation of a tetracyclic catechol. *Anal Biochem* 1993; **214**: 442–451.
14. Miller FJ Jr, Griendling KK: Functional evaluation of non-phagocytic NAD(P)H oxidases. *Methods Enzymol* 2002; **353**: 220–233.
15. Otsuka S, Sugano M, Makino N, Sawada S, Hata T, Niho Y: Interaction of mRNAs for angiotensin II type 1 and type 2 receptors to vascular remodeling in spontaneously hypertensive rats. *Hypertension* 1998; **32**: 467–472.
16. Goto M, Mukoyama M, Sugawara A, *et al*: Expression and role of angiotensin II type 2 receptor in the kidney and mesangial cells of spontaneously hypertensive rats. *Hypertens Res* 2002; **25**: 125–133.
17. Schiffrin EL: The many targets of aldosterone. *Hypertension* 2004; **43**: 938–940.
18. Braun S, Losel R, Wehling M, Boldyreff B: Aldosterone rapidly activates Src kinase in M-1 cells involving the mineralocorticoid receptor and HSP84. *FEBS Lett* 2004; **570**: 69–72.
19. Takeda Y, Miyamori I, Yoneda T, Iki K, Hatakeyama H, Takeda R: Gene expression of 11 beta-hydroxysteroid dehydrogenase in the mesenteric arteries of genetically hypertensive rats. *Hypertension* 1994; **23**: 577–580.
20. Sato A, Suzuki Y, Shibata H, Saruta T: Plasma aldosterone concentrations are not related to the degree of angiotensin-converting enzyme inhibition in essential hypertensive patients. *Hypertens Res* 2000; **23**: 25–31.
21. Cohn JN, Anand IS, Latini R, Masson S, Chiang YT, Glazer R: Sustained reduction of aldosterone in response to the angiotensin receptor blocker valsartan in patients with chronic heart failure: results from the Valsartan Heart Failure Trial. *Circulation* 2003; **108**: 1306–1309.
22. Park JB, Touyz RM, Chen X, Schiffrin EL: Chronic treatment with a superoxide dismutase mimetic prevents vascular remodeling and progression of hypertension in salt-loaded stroke-prone spontaneously hypertensive rats. *Am J Hypertens* 2002; **15**: 78–84.
23. Nakazono K, Watanabe N, Matsuno K, Sasaki J, Sato T, Inoue M: Does superoxide underlie the pathogenesis of hypertension? *Proc Natl Acad Sci USA* 1991; **88**: 10045–10048.
24. Hornig B, Landmesser U, Kohler C, *et al*: Comparative effect of ACE inhibition and angiotensin II type 1 receptor antagonism on bioavailability of nitric oxide in patients with coronary artery disease: role of superoxide dismutase. *Circulation* 2001; **103**: 799–805.
25. Brahmajothi MV, Campbell DL: Heterogeneous basal expression of nitric oxide synthase and superoxide dismutase isoforms in mammalian heart: implications for mechanisms governing indirect and direct nitric oxide-related effects. *Circ Res* 1999; **85**: 575–587.
26. Didion SP, Ryan MJ, Didion LA, Fegan PE, Sigmund CD, Faraci FM: Increased superoxide and vascular dysfunction in CuZnSOD-deficient mice. *Circ Res* 2002; **91**: 938–944.
27. Chaudiere J, Ferrari-Iliou R: Intracellular antioxidants: from chemical to biochemical mechanisms. *Food Chem Toxicol* 1999; **37**: 949–962.
28. Chang MS, Yoo HY, Rho HM: Transcriptional regulation and environmental induction of gene encoding copper- and zinc-containing superoxide dismutase. *Methods Enzymol* 2002; **349**: 293–305.
29. Schupp M, Janke J, Clasen R, Unger T, Kintscher U: Angiotensin type 1 receptor blockers induce peroxisome proliferator-activated receptor-gamma activity. *Circulation* 2004; **109**: 2054–2057.
30. Zalba G, San Jose G, Moreno MU, *et al*: Oxidative stress in arterial hypertension: role of NAD(P)H oxidase. *Hypertension* 2001; **38**: 1395–1399.
31. Csonka C, Pataki T, Kovacs P, *et al*: Effects of oxidative stress on the expression of antioxidative defense enzymes in spontaneously hypertensive rat hearts. *Free Radic Biol Med* 2000; **29**: 612–619.
32. Marklund SL: Extracellular superoxide dismutase and other superoxide dismutase isoenzymes in tissues from nine mammalian species. *Biochem J* 1984; **222**: 649–655.